

Medical Image Analysis
Report Project 1
Fabian Prada
Team 7 .Teammate Rob Grupp

1 Abstract

In this project we present a method to identify microcalcification in mammograms. Our method performs an initial breast segmentation, based in active contours, and a microcalcification detection using a local region growing algorithm. Classification of normal/unnormal images is based on the maximum density of microcalcifications candidates.

2 Introduction

For a comprehensive study of mammographic imaging we refer the reader to [3]. For classification of microcalcifications we refer to [1]. Microcalcifications are perceived as clusters of small pixel blocks with large intensity values. Detecting such clusters in a robust way involves a broad set of techniques from image processing.

In order to improve the contrast (visibility) of the microcalcification several filtering techniques have been suggested. Probably, the simplest approach to enhance the contrast between microcalcifications and neighbouring pixels are intensity remapping like gamma correction ($a \leftarrow a^\gamma$) or linear filtering like laplacian sharpenning ($I \leftarrow (id + \lambda\Delta)I$). Other techniques compute new intensity values by matching a target histogram, and some others grow regions of similarity and increase the intensity value separation of surrounding pixels.

Since microcalcifications are located in the fibrograndular tissue, an accurate segmentation of this region is also important. Segmentation of the breast is usually assisted by morphological operators to remove pixel block exterior to breast. After this, the boundary of the breast is estimated using deformable models like active countours [4].

Once the breast has been detected the ROI can be further limited by separating the fibrograndular tissue from the pectoral muscle. The Hough Transform and Gabor Filters are common techniques applied for this task.

Traditional approaches identify candidate microcalcifications regions and classify them according to shape and size.

3 Approach

Our method to detect microcalcification can be decomposed in three major steps:

1. Candidate region pruning.
2. Candidate region detection.
3. Candidate region labeling.

3.1 Candidate Region Pruning

The goal of our pruning method is to discard all regions in the image that do not belong to the breast or are unlikely to contain microcalcifications.

First, we segment the breast by identifying a contour around it. This part of the project was implemented by Rob following [2]. The result of the segmentation is presented in Figure 1.

Since microcalcification tends to concentrate in the central region of the fibroglandular tissue, we add a second masking pass based on the distance of pixels to the image boundary. Ideally, from a large collection of training images we could compute for each pixel location the probability of being a microcalcification. Our boundary based masking strategy is just a proxy to candidate region pruning based in a thresholding of such probability density function.

3.2 Candidate Region Detection

Our second step consists of finding windows in the image that are likely to contain microcalcifications.

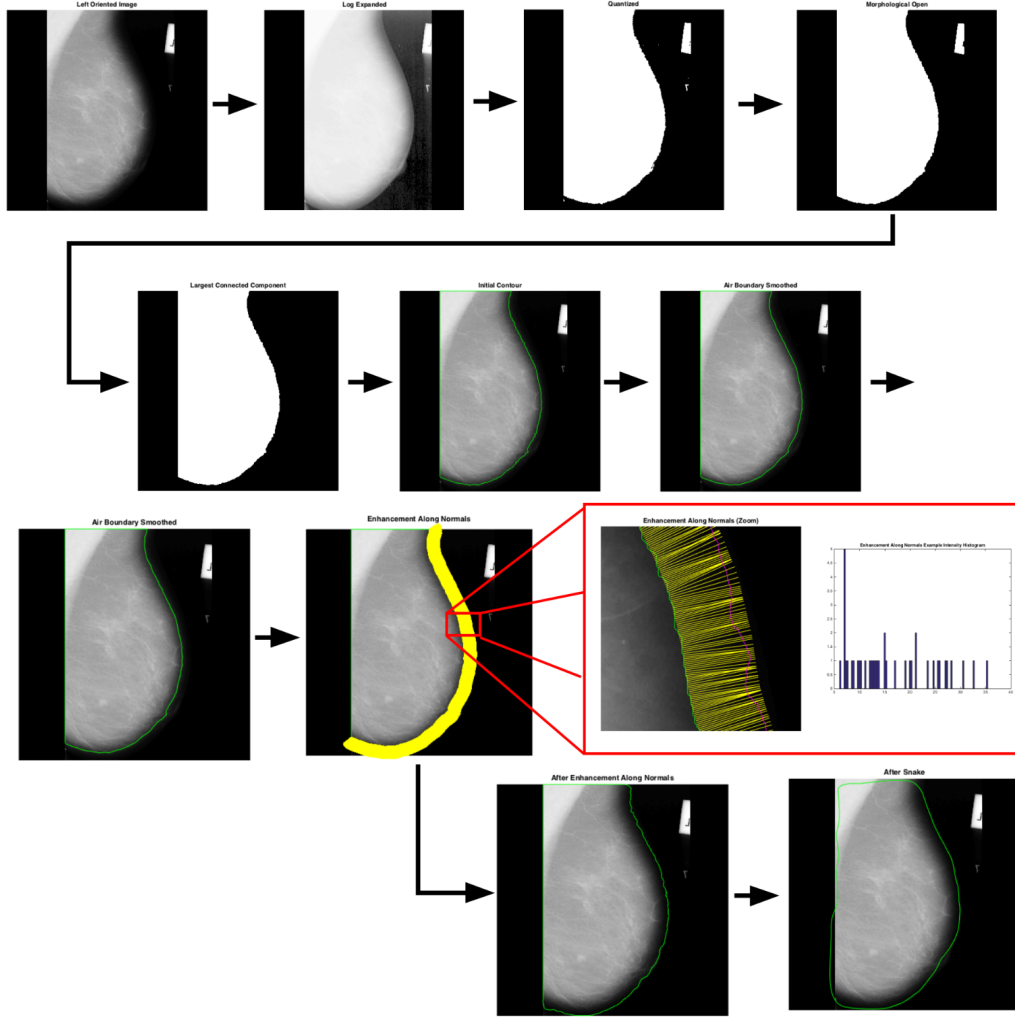


Figure 1: Breast Segmentation. Image Courtesy of Rob Grupp.

First, we identify pixels in the image that are maxima within certain windows radius and with value above certain threshold (we take $r = 3$ and $v = 0.65$, resp.). These pixels are our initial "microcalcifications centers", and are observed as white spots in Figure 3.

Then, we proceed to do a *simultaneous local region growing* taking as

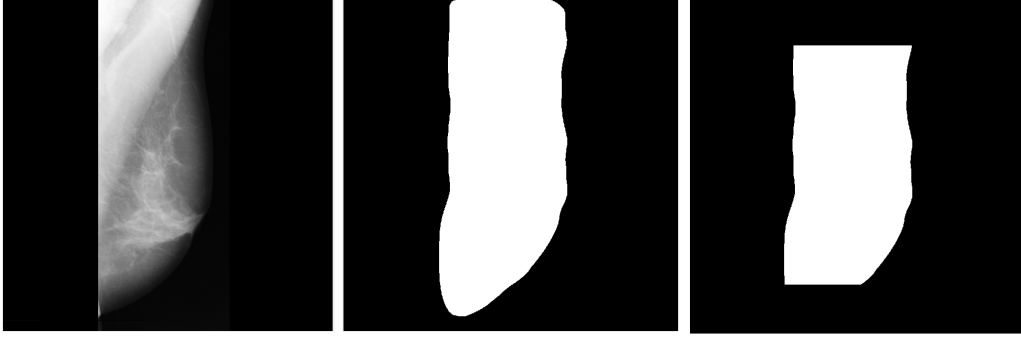


Figure 2: Breast Mask. From left to right: input, segmentation result, and additional boundary based masking.

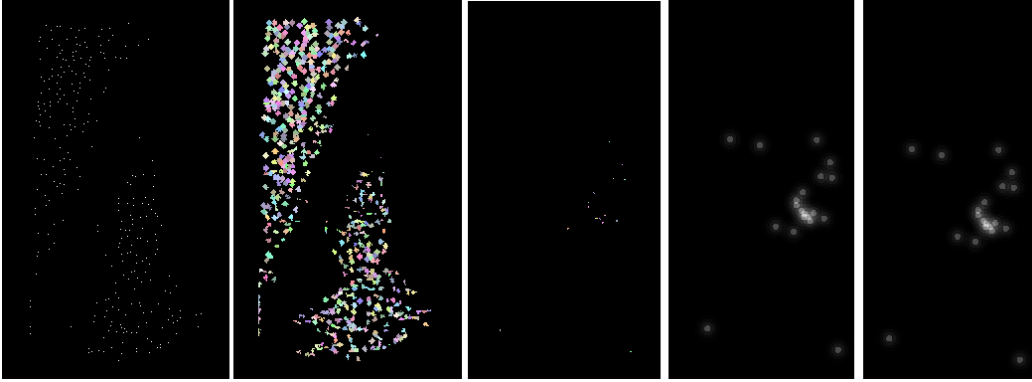


Figure 3: Candidate detection. From left to right: local maxima, region growing maxima, region size thresholding, density score, cumulative density score

seeds the previously identified "microcalcifications centers". At each iteration, region growing add a new pixel p to the region i -th if $|v(p) - v(s_i)| < \tau$, and p has not been added to a previous region. We grow the regions to a maximum of 10 pixel diameter. In this way, we get a collection of disjoint "microcalcifications regions" as observed in the second image of Figure 3.

Our next step is to apply a morphological filter: each microcalcifications region is expected to be small and isotropic (i.e., large masses or elongated

shapes are not common). Our morphological filter is just a tresholding on the size of the microcalcifications (we discard regions with more than 9 pixels). The regions remaining after this pruning are observed in the third image of Figure 3.

Our last step consists on identifying "microcalcifications clusters". We define the score of a pixel, $s(p)$, to be a cummulative sum of densities of valid "microcalcifications centers". Define the set,

$$X(p, r) = \{x : |x - p| < r \text{ and } x \text{ is a valid MC center}\},$$

we set the score for a pixel p to be the center of a microcalcification cluster as,

$$s_\tau(p) = \sum_{r=1}^{50} \frac{|X(p, r)|}{r^2}$$

The value of the pixel scores are shown in the fourth image of Figure 3, for $\tau = 0.96$.

The size of the microcalcification regions depends on the region growing parameter τ . In order to increase the robustness of our algorithm we run the score computation for different values of τ (we use $0.93 : 0.01 : 0.97$), and take as final score the average of the results. Our final "microcalcifications score" at each pixel is,

$$s(p) = \frac{1}{k} \sum_k s_{\tau_k}(p)$$

3.3 Candidate Region Labeling

After computing the "microcalcifications scores" of an image we identify the best microcalcification candidate as the pixel with maximum score. By comparing the maximum score among normal images and images with microcalcifications, we identified $\alpha = 0.16$ to be an appropriate threshold to classify between normal images (maximum score less than α) and images with microcalcifications (maximum score larger than α). We must notice that a prefect separation was not obtained (we got around 90% of classification accuracy)

from the training data, and additional features must be explored in order to get better classification.

Finally, for each of the microcalcification candidates we need to identify the radius of the microcalcification cluster (we take as cluster center the coordinates of the pixel itself). We define the set,

$$Y(p, r) = \{y : |y - p| < r \text{ and } y \text{ is a in valid MC region}\},$$

The difference respect to the previously defined set X , is that Y is not only counting the pixels that are microcalcification centers in a neighbourhood of p , but also the pixels covered after the region growing (we use a fixed $\tau = 0.97$). The optimal cluster radius is given by,

$$\operatorname{argmax}_{r \in 10:5:50} \frac{Y(p, r)}{r}$$

4 Results

The following table summarize the results we obtained on the training data,

Image Name	Score	(x,y,r) GT	(x,y,r) Detected
Microcalcifications Images			
213	0.612	477 505 45	462 536 45
223	0.841	502 543 29	512 540 25
231	0.548	421 487 44	395 469 10
238	0.892	522 472 17	522 481 20
239	0	379 270 40	-1 -1 -1
241	1	571 347 38	570 356 35
248	0.872	378 424 10	381 424 15
252	0.639	439 658 23	427 644 50
253	0	291 461 28	-1 -1 -1
256	0	400 541 37	258 557 50
Normal Images			
52	1	-1 -1 -1	-1 -1 -1
54	1	-1 -1 -1	-1 -1 -1
56	1	-1 -1 -1	-1 -1 -1
60	1	-1 -1 -1	-1 -1 -1
62	0	-1 -1 -1	366 764 10
88	1	-1 -1 -1	-1 -1 -1
94	1	-1 -1 -1	-1 -1 -1
96	1	-1 -1 -1	-1 -1 -1
100	0	-1 -1 -1	360 307 10
106	1	-1 -1 -1	-1 -1 -1

For images with microcalcifications our method was correct in 60% of the cases. Despite the correct identification of microcalcifications we observe large deviation between the predicted center/radius and the ground-truth. This however seems very subjective since manually labeling of the center and radius of these structures is prone to user bias. For normal images the accuracy of classification was 80%.

We run our training evaluation in an Intel Core i7 5700HQ CPU. Processing a single image took around 4 seconds.

5 Team Evaluation

In the contest section our team obtained a score of 0.562 which seems consistent with the results previously discussed. We identify three possible explanations of why a better result was not obtained. The way we select the optimal parameters for our method was based in a training set where half the images were normal and half had microcalcifications, this was not the case of the testing data. Possibly setting parameters more "tolerant" with microcalcification candidates would have produced better results. Another reason is that the location and radius of the microcalcifications cluster produced by our method seem to be suboptimal. A more thorough identification of these parameters would have improved our result. Finally, our classification of normal/unnormal images is based on a single feature classifier. Learning more features to assist the classification should make the algorithm more robust. Rob did a great job on implementing a surprisingly fast breast segmentation so he deserves at least 2 points. I worked on the microcalcification detection and my local region growing algorithm was an interesting approach that was not considered by other groups, so I think I also deserve 2 points.

6 Conclusions

The detection of microcalcification is a challenging task that requires a thorough image analysis. We obtained results slightly above the average for images with microcalcifications and very good results for normal images. The main weakness of our approach is probably the lack of a robust classifier. Identifying more features for the candidate regions and learning statistics from other images seems the right direction to improve our results.

References

- [1] Horsch A. Elter M. Cadx of mammographic masses and clustered microcalcifications: a review. *Med. Phys.*, 2009.
- [2] R. J. Ferrari, A. F. Frère, R. M. Rangayyan, J. E. L. Desautels, and R. A. Borges. Identification of the breast boundary in mammograms using active contour models. *Medical and Biological Engineering and Computing*, 42(2):201–208, 2004.

- [3] Maryellen L. Giger. Medical imaging 2008: Computer-aided diagnosis. *Proceedings of Spie*.
- [4] Michael Kass, Andrew Witkin, and Demetri Terzopoulos. Snakes: Active contour models. *International Journal of Computer Vision*, 1(4):321–331, 1988.